Mechanistic Insights into Arrhythmogenic Right Ventricular Cardiomyopathy Caused by Desmocollin-2 Mutations

Cardiovascular Research (2011) **90**, 77–87
doi:10.1093/cvr/cvq353

Mechanistic insights into arrhythmogenic right ventricular cardiomyopathy caused by desmocollin-2 mutations

Katja Gehmlich[1]*†, Petros Syrris[1], Emma Peskett[1], Alison Evans[1], Elisabeth Ehler[2], Angeliki Asimaki[3], Aris Anastasakis[4], Adalena Tsatsopoulou[5], Apostolos-Ilias Vouliotis[4], Christodoulos Stefanadis[4], Jeffrey E. Saffitz[3], Nikos Protonotarios[5], and William J. McKenna[1]

[1]Institute of Cardiovascular Science, University College London, London, UK; [2]The Randall Division of Cell and Molecular Biophysics and the Cardiovascular Division, King's College London, BHF Centre of Research Excellence, London, UK; [3]Department of Pathology, Beth Israel Deaconess Medical Centre, Harvard Medical School, Boston, MA, USA; [4]Unit of Inherited Cardiovascular Diseases, Heart Center of the Young and Athletes, First Department of Cardiology, University of Athens, Athens, Greece; and [5]Yannis Protonotarios Medical Center, Naxos Island, Greece

Received 10 May 2010; revised 3 November 2010; accepted 4 November 2010; online publish-ahead-of-print 9 November 2010

Time for primary review: 28 days

Aims Recent immunohistochemical studies observed the loss of plakoglobin (PG) from the intercalated disc (ID) as a hallmark of arrhythmogenic right ventricular cardiomyopathy (ARVC), suggesting a final common pathway for this disease. However, the underlying molecular processes are poorly understood.

Methods and results We have identified novel mutations in the desmosomal cadherin desmocollin 2 (DSC2 R203C, L229X, T275M, and G371fsX378). The two missense mutations (DSC2 R203C and T275M) have been functionally characterized, together with a previously reported frameshift variant (DSC2 A897fsX900), to examine their pathogenic potential towards PG's functions at the ID. The three mutant proteins were transiently expressed in various cellular systems and assayed for expression, processing, localization, and binding to other desmosomal components in comparison to wild-type DSC2a protein. The two missense mutations showed defects in proteolytic cleavage, a process which is required for the functional activation of mature cadherins. In both cases, this is thought to cause a reduction of functional DSC2 at the desmosomes in cardiac cells. In contrast, the frameshift variant was incorporated into cardiac desmosomes; however, it showed reduced binding to PG.

Conclusion Despite different modes of action, for all three variants, the reduced ability to provide a ligand for PG at the desmosomes was observed. This is in agreement with the reduced intensity of PG at these structures observed in ARVC patients.

Keywords Arrhythmogenic right ventricular cardiomyopathy • Desmocollin-2 • Desmosome • Functional studies • Mutation

1. Introduction

Arrhythmogenic right ventricular cardiomyopathy (ARVC) is a heart muscle disorder associated with heart failure, ventricular arrhythmias,[1,2] and sudden death.[3] Familial disease occurs in 30–50% of the cases with usually autosomal-dominant inheritance. Mutations in five cardiac desmosomal genes have been identified,[2] founding the hypothesis that ARVC is a 'disease of altered cell–cell adhesion'.

* Corresponding author. Tel: +44 1865 234902, fax: +44 1865 234681, Email: katja.gehmlich@cardiov.ox.ac.uk

† Present address. Department of Cardiovascular Medicine, University of Oxford, Level 6, West Wing, John Radcliffe Hospital, Headley Way, Headington, Oxford OX3 9DU, UK.

The desmosomes are specialized cell–cell contact structures within the intercalated disc (ID), which allow the heart to withstand mechanical strain during contractile cycles. In these structures, the desmosomal cadherins desmoglein-2 (DSG2) and desmocollin-2 (DSC2) link neighbouring cells via interactions with their extracellular cadherin domains.[4] The intracellular portions of both proteins interact with plakoglobin (PG) and plakophilin-2 (PKP2), which in turn bind desmoplakin (DSP), therefore providing a link to intermediate filaments.[5]

At the histological level, ARVC is characterized by a progressive replacement of cardiomyocytes by fibro-fatty infiltrates.[6] Recently, the loss of PG immunoreactivity from the ID has been suggested as a highly specific and sensitive marker for the disease.[7] In this study, almost all cardiac tissues from ARVC patients showed a loss of PG from the ID, independent of the affected gene. Equally important, this loss of PG staining was not observed in tissues of other cardiac conditions. Although this highlights the diagnostic value of this test for defining ARVC in patients, the molecular changes underlying the phenomenon are yet to be identified.

So far, functional studies have mainly focused on the role of DSP, PKP2, and PG to elucidate potential patho-mechanisms of ARVC.[8–11] Mutations in both cardiac desmosomal cadherins, DSG2 and DSC2, also contribute to the disease.[2,12–14] The crucial function of DSC2 for the heart was demonstrated by knock-down experiments in the zebrafish model.[15] DSC2 is expressed as two different splice variants with different Carboxy-termini.[16] The DSC2a isoform has a larger cytoplasmic domain than the DSC2b isoform; however, the differential functions of the two isoforms in the myocardium are not well characterized. Interestingly, the DSC2 A897fsX900 variant[17] only affects the DSC2a, but not the DSC2b isoform. This variant was initially found in ARVC families, where it co-segregated with disease (referred to as DSC2 E896fsX900 in Syrris *et al.*[17]). However, it has now also been identified in apparently healthy individuals,[18] disputing its causative role in ARVC.

Here, we describe four novel mutations in DSC2 causing ARVC. Two of them are predicted to be non-functional alleles. In contrast, the characteristics of the two missense mutations are to be defined. To do so, we perform functional studies on these two mutations and also include the previously described DSC2 A897fsX900 variant in our tests. Our experiments demonstrate a pathogenic potential of all three mutations analysed. Despite the different properties of the mutant proteins, one common feature was observed in all cases: a reduced ability to retain PG at the cardiac desmosomes. This may play a pivotal role in the pathogenesis of the disease.

2. Methods

2.1 Clinical evaluation and mutation screening

Informed consent was obtained from the participating individuals and the study was approved by the Joint UCL/UCLH Ethics Committees, Research and Development Directorate (ref. no. 03/0306). The investigation conforms with the principles outlined in the Declaration of Helsinki. Genetic screening of DSP, PG, PKP2, DSG2, and DSC2 by direct sequencing and clinical evaluation were performed as described previously.[19] The latter included 12-lead electrocardiogram (ECG), signal-averaged ECG with 40 Hz filter, two-dimensional echocardiography, maximal exercise testing, ambulatory ECG monitoring, and coronary angiography (where needed). The diagnosis of ARVC was based on the recent revision of the original criteria proposed by the International Task Force of the European Society of Cardiology and International Society and Federation of Cardiology (ESC/ISFC).[20]

2.2 Immunohistochemical analysis of myocardial tissue

Myocardial tissue of Patient 55.2 was probed for changes in the localization of desmosomal proteins by immunofluorescence and confocal microscopy as described[21] using the following antibodies: polyclonal rabbit anti-connexin 43 (Cx43) (Sigma), monoclonal mouse anti-PG (Sigma), polyclonal rabbit anti-DSP (SeroTec), monoclonal mouse anti-N-cadherin (Sigma), and monoclonal mouse anti-PKP2 (BioDesign).

2.3 Generation of cDNA constructs

A full-length human DSC2a wild-type (WT) cDNA was kindly provided by Prof. W. Franke (German Cancer Research Center, Heidelberg, Germany) and cloned into pEGFP-N1 (Clontech) and pCDNA3 (Invitrogen). The mutations (R203C, T275M, and A897fsX900) were introduced by site-directed mutagenesis (Quikchange kit, Stratagene). Human sequences corresponding to cytoplasmic regions of DSC2a WT (aa 716–901), A897fsX900 (aa 716–899), DSC2b (aa 716–847), and DSG2 (aa 635–842) were cloned into pGEX6P1 (GE Healthcare) and mammalian expression vector pEBG[22] (a kind gift of Dr Alan Whitmarsh, University of Manchester, UK).

2.4 Antibodies

The following antibodies were for functional studies: a mouse monoclonal antibody (mAB) against green fluorescent protein (GFP, Roche), desmocollin2/3 mAB (clone 7G6, Zymed), PG mAB (clone 15/γ-Catenin BD Biosciences), desmoglein1/2 (clone DG3.10, Progen), PKP2 mAB (multi-epitope cocktail, Progen), giantin mAB (Golgi apparatus marker[23]). β-Catenin (Sigma), DSC2 (Sigma, Prestige Antibody Ab2, HPA012615) and DSP (Serotec) polyclonal rabbit, and anti-GST polyclonal goat antibodies were also used. Sheep-anti-mouse IgG antibody (GE Healthcare) and rabbit-anti-goat IgG antibody (Pierce), both conjugated to horseradish peroxidase, were used for the detection of primary antibodies in western blotting.

2.5 Cell culture and transfections

COS-1 cells were cultured and transfected with Escort IV (Sigma) as described,[24] using 7.5 μg of each DNA construct in 10 cm dishes.

The atrial cell line HL-1 (a kind gift of Dr R. Breckenridge, Centre for Clinical Pharmacology, University College London, UK) was cultured in Claycomb medium (Sigma), supplemented with 10% foetal bovine serum (Sigma), 2 mM L-glutamine (Gibco), 100 U/mL penicillin, 100 μg/mL streptomycin (Gibco), and 100 μM noradrenalin (Sigma). HL-1 cells were transfected with 4 μg of DNA and Lipofectamine 2000 (Invitrogen) according to the manufacturer's instructions.

Primary cultures of neonatal rat cardiomyocytes (NRC) were established using the Neonatal Cardiomyocyte Isolation System from Worthington (Lakewood, NJ, USA). The use of the neonatal rats was in accordance with the NIH guidelines. The cells were plated, maintained, and transfected on day 1 after plating using 5 μg of DNA and JetPrime transfection reagent (Autogen Bioclear) as described.[13] All transfected cells were analysed for expression of the recombinant proteins 48 h after transfection. Indirect immunofluorescence and confocal microscopy were performed as described.[13]

2.6 GST-pulldown assays

Expression of GST fusion proteins in BL21 Codon Plus strain (Stratagene) and purification with glutathione–sepharose beads (GE Healthcare) has been described elsewhere.[13] Protein-loaded beads were incubated with pre-cleared adult rat heart lysate (350 μg total protein) in GST-pulldown buffer for 1 h on ice. After washing three times with GST-pulldown buffer,

the bound proteins were eluted with two-fold SDS sample buffer. GST fusion proteins were analysed by SDS–PAGE and visualized with Instant-Blue (Generon), and western blotting was performed to probe for bound PG and PKP2.

Detailed descriptions of the experiments (including buffer solution compositions) can be found in the Supplementary material online.

3. Results

3.1 Identification of novel DSC2 mutations in ARVC patients

Genetic screening of DSC2 revealed a single heterozygous change in exon 5 (c.607 C > T) in a Caucasian ARVC patient (family 35), coding for an arginine to cysteine missense change at position 203 (DSC2 R203C, *Figure 1A* and see Supplementary material online, *Table S1*). In addition, a further heterozygous missense change in DSP (c.5498 A > T coding for E1833V) was identified in the index patient (35.1). A recent study has suggested a frequency of 1.5% for this polymorphism.[25] In the same family, the DSC2 R203C mutation was also found in Individual 35.3, who was negative for the DSP E1833V variant. He had a borderline diagnosis for ARVC[20] (see Supplementary material online, *Table S1*). His available siblings (35.2 and 35.4) were negative for the DSC2 mutation and clinically normal; one of them (35.4) carried the DSP E1833V variant.

In another ARVC patient (37.1), a homozygous change in exon 7 (c. 824 C > T) was found, predicting a threonine to methionine missense change at position 275 (DSC2 T275M, *Figure 1B*). Both daughters of the index patient (37.2 and 37.3) were heterozygous for the DSC2 T275M mutation and asymptomatic. One of them (37.3) was available for clinical testing and clinically normal.

In family 53, a heterozygous deletion of one base pair was found in exon 6 (c. 685 delC), which predicts a premature Stop codon at position 229 (DSC2 L229X, *Figure 1C*). The index patient (53.1) also carried a benign, heterozygous PKP2 A372P variant.[26] His brother (53.2) also fulfilled diagnostic criteria for ARVC in the presence of the DSC2 L229X mutation, whereas the son (53.3) was clinically unaffected in the presence of the mutation.

Finally, a two-base pair deletion was found in exon 9 (c.1112_1113delTG) in family 55 (Individual 55.1). This heterozygous change predicts a frameshift at amino acid 371, leading to a premature stop at position 378 (DSC2 G371fsX378, *Figure 1D*). The son (55.2) had died suddenly at the age of 35 and diagnosis of ARVC was confirmed histologically at post-portem (see Supplementary material online, *Figure S5A*) in the presence of the mutation. His sister (55.3) was negative for the DSC2 mutation and clinically normal. The sister of the index patient (55.4) did not fulfil diagnostic criteria for ARVC in the presence of the mutation.

None of the DSC2 mutations was found in 200 control individuals. No further changes were found in PKP2, PG, DSG2, or DSP in these families.

3.2 Functional studies on ARVC-associated DSC2 mutations

The novel mutations DSC2 L229X and DSC2 G371fsX378 are predicted to generate non-functional alleles: The truncated proteins, if expressed at all, cannot be anchored in the plasma membrane (*Figure 2A*). In contrast, the newly identified missense mutations DSC2 R203C and DSC2 T275M only change a single amino acid in the extracellular domains of the protein (*Figure 2A*), whereas the DSC2 A897fsX900 variant also only affects a small portion of the cytoplasmic domain (namely the last five amino acids of the DSC2a isoform, *Figure 2A*; see Supplementary material online, *Figure S1A*).

We speculated that these different variants may contribute to the same disease mechanism. To understand the pathogenic action of DSC2 R203C, DSC2 T275M, and DSC2 A897fsX900, all three mutations were introduced into a DSC2a cDNA and functionally characterized.

3.3 Impaired proteolytic processing of N-terminal DSC2 mutations

The mutant proteins were expressed in COS-1 cells and analysed by western blotting in comparison to their WT counterpart: the DSC2 WT protein was detected predominantly in its cleaved, mature form ('M' in *Figure 2B*, ~90% *Figure 2C*) and only small amounts of the un-cleaved precursor form could be detected ('P' in *Figure 2B*, ~10%, *Figure 2C*; see Supplementary material online, *Figure S2*). The same ratio was observed for the A897fsX900 mutation. In contrast, the DSC2 R203C protein was exclusively detected in the unprocessed pro-protein form, and the DSC2 T275M showed a significantly higher ratio of pro-protein to mature protein (*Figure 2B* and *C*; see Supplementary material online, *Figure S2*).

These findings suggest that while the vast majority of DSC2 WT and A897fsX900 are correctly processed into their active form, the T275M protein is impaired in this maturation process and the R203C protein completely fails to undergo it.

3.4 Partial or severe defects in desmosomal localization of N-terminal DSC2 mutations

As a next step, we investigated the localization of the three DSC2 mutants in the cardiac cell line HL-1. Transiently transfected DSC2 WT showed predominant localization at cell borders (*Figure 3*; also see Supplementary material online, *Figure S1B*); higher magnification showed a dotted appearance of the DSC2 protein at the sites of cell–cell contacts, indicating incorporation into desmosomes.[27] Depending on the expression level, part of the over-expressed protein was additionally found in the Golgi apparatus and in intracellular vesicles. The localization of the DSC2 A897fsX900 variant was similar to WT protein, with a slight shift from cell border to Golgi apparatus localization (*Figure 3B*). This suggests that this variant can be incorporated into desmosomes. The DSC2 R203C protein failed to localize at the cell borders and was absent from desmosomal structures. Instead, it was diffuse or localized in vesicles throughout the cytoplasm of the HL-1 cells. Although the DSC2 T275M protein was able to localize in the desmosomes, a shift towards vesicular and Golgi apparatus localization was observed (*Figure 3B*).

In primary cardiomyocytes, DSC2 WT was almost exclusively found at the ID, where it co-localized with recognized ID markers such as β-catenin (*Figure 4*). In agreement with our HL-1 studies, the DSC2 A897fsX900 protein was also found to be normally incorporated into the ID (*Figure 4B*). Only a very small fraction of DSC2 R203C was targeted to the ID structures, most of the protein was found in cytoplasmic vesicles (*Figure 4*; see Supplementary material online, *Figure S3*). The DSC2 T275M mutation was found at the ID, although to a lesser extent than the WT protein, and showed additional vesicular localization in the cytoplasm.

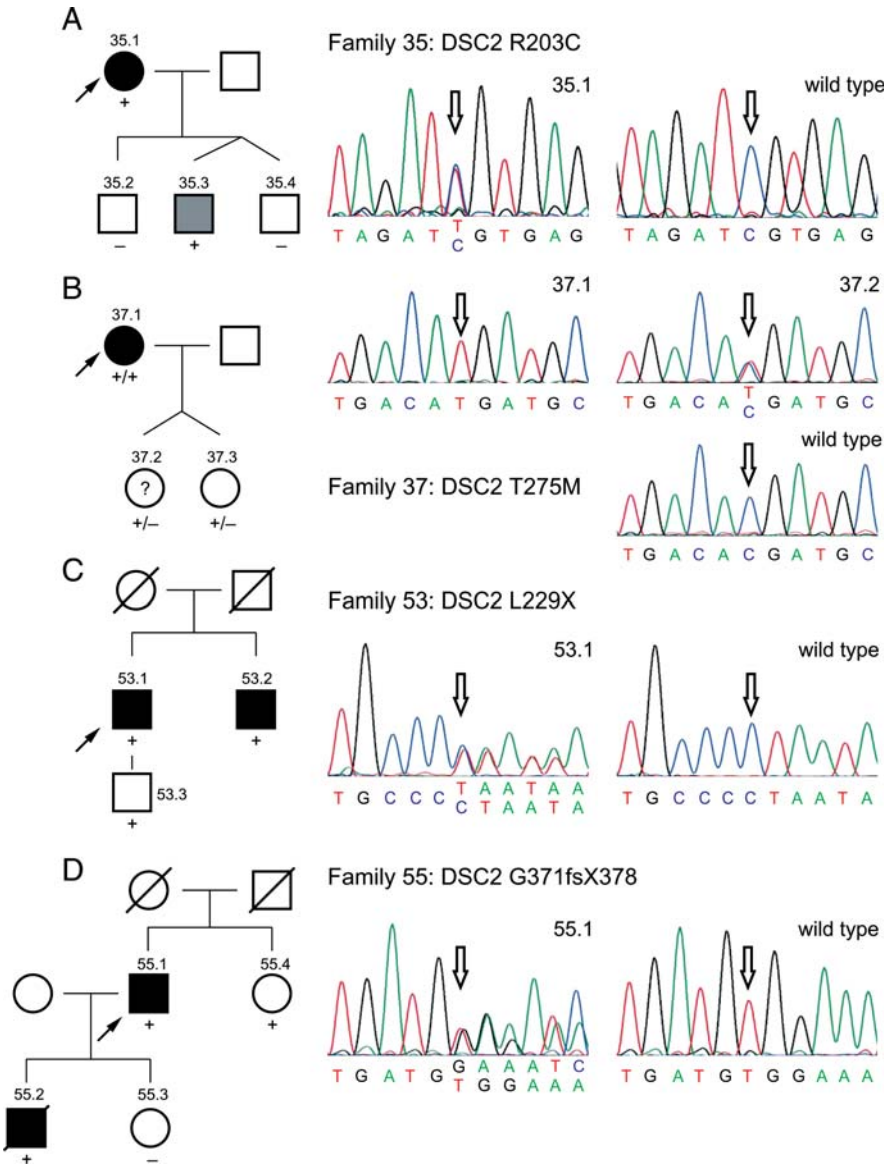

Figure 1 Identification of novel mutations in DSC2 in Caucasian families. Pedigrees of the families with novel DSC2 mutations: black symbols, fulfils diagnostic criteria for ARVC[20]; white symbols, does not fulfil TFC; grey symbol, borderline ARVC diagnosis; question mark, unknown disease status. Slanted bars, deceased individuals; squares, males; circles, females; plus (+) and minus (−) indicate the presence or absence of the DSC2 mutation; arrow, index patient; for details, see Supplementary material online, *Table S1*. The pedigrees of the families are shown on the left, the sequence electropherograms on the right (open arrows indicate mutations in comparison to WT individuals). (*A*) A heterozygous DSC2 R203C mutation in family 35 (C → T change at nucleotide position 607). (*B*) Family 37: Individual 37.1 is homozygous for DSC2 T275M (C → T change at nucleotide position 824), whereas Individual 37.2 is heterozygous for the same change. (*C*) In family 53, a heterozygous deletion of C at nucleotide position 685 causes DSC2 L229X. (*D*) A heterozygous two-base pair deletion was identified in family 55 (c.1112_1113delTG), resulting in DSC2 G371fsX378.

3.5 The DSC2a A897fsX900 variant is impaired in binding to PG

Our localization studies demonstrated that the DSC2 A897fsX900 variant is incorporated into the desmosomes similar to the DSC2 WT protein, whereas the N-terminal missense mutations are impaired or defective in this process. Therefore, the DSC2 A897fsX900 variant appears to have different characteristics, and any pathogenic potential of this variant should be an adverse action at the desmosomes, most likely by affecting binding properties of the intracellular, cytoplasmic domain, which links DSC2 to PG and PKP2.[5]

To explore the nature of this variant in more detail, we performed binding assays to investigate how the cytoplasmic tails of all cardiac desmosomal cadherins, namely DSC2a, DSC2b, and DSG2, contribute to binding PG and PKP2 (*Figure 5A*). Using rat heart lysates, GST fusion proteins of all three pulled out PKP2, whereas only DSC2a and DSG2 bound to PG. This suggests that the binding sites of PG and PKP2 might be distinct. Interestingly, the DSC2 A897fsX900 variant bound normally to PKP2; however, its binding to PG was reduced by ∼50%.

To confirm these findings, GST fusion proteins of the cytoplasmic tail of DSC2a WT and A897fsX900 were expressed in COS-1 cells

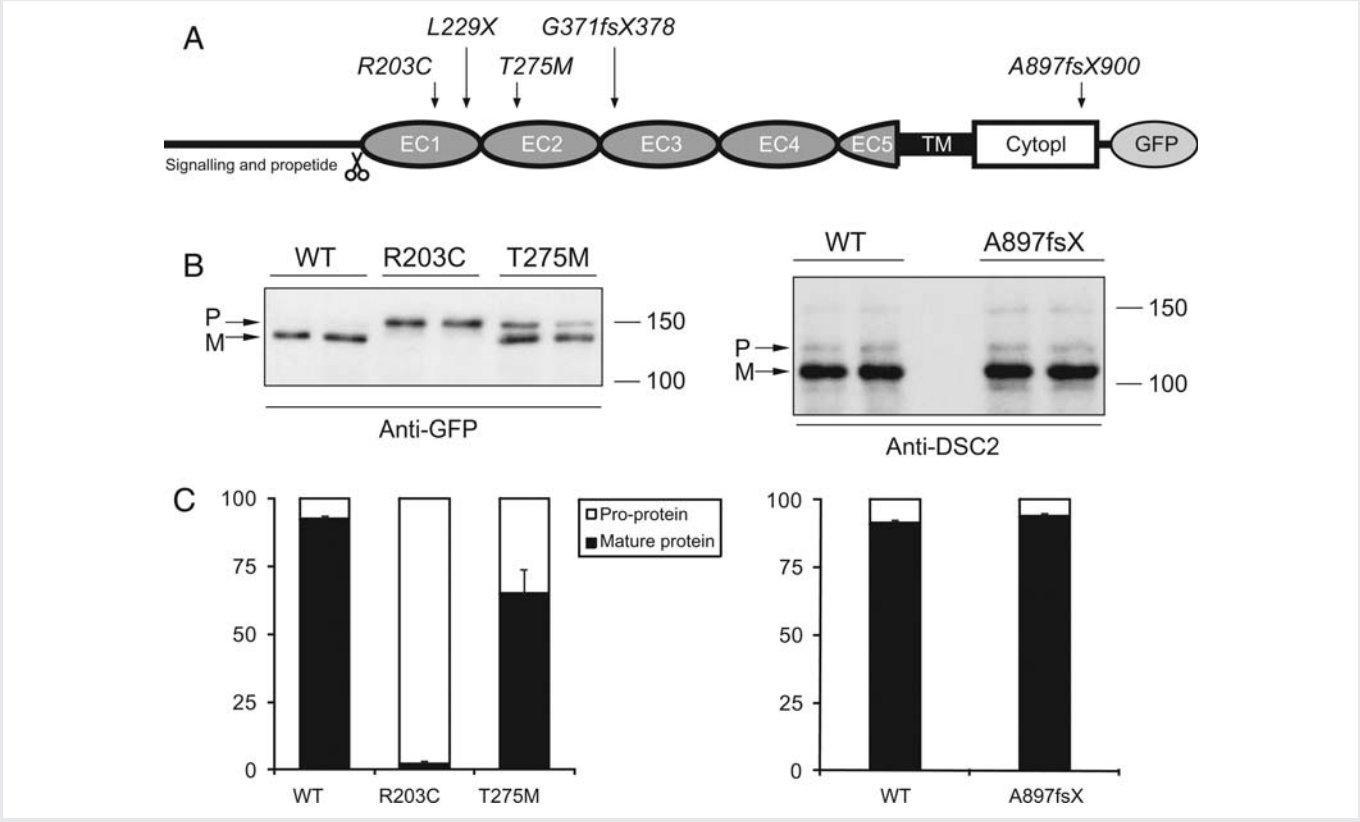

Figure 2 DSC2 R203C and T275M display processing defects. (*A*) Position of the newly identified mutations and the A897fsX900 variant in DSC2a (modified from Awad *et al.*[2]). The cleavage site (scissors symbol) during proteolytic maturation is indicated, also the five extracellular cadherin domains (EC), the transmembrane region (TM), and the cytoplasmic domain (cytopl). The position of the GFP tag used in some experiments is also indicated. (*B*) Western blot of DSC2a WT and the R203C and T275M mutant proteins (using GFP fusion proteins), as well as of DSC2a WT and the A897fsX900 variant (using tag-free constructs). The positions of pro-protein form (P) and mature protein (M) are indicated for DSC2 WT. (*C*) Quantification of pro-protein to mature protein ratios by densitometry. The results of one representative experiment are shown as mean ratio ± standard deviation (in total, four independent experiments). Results of Student's *t*-test: R203C vs. WT, $P < 0.001$; T275M vs. WT, $P < 0.05$; A897fsX900 vs. WT, $P = 0.62$ (not significant).

and assayed for binding to endogenous PKP2 and PG. As shown in *Figure 5B*, the DSC2a A897fsX900 protein showed a dramatically reduced binding to PG, whereas binding to PKP2 was only mildly affected.

Binding to DSP was assessed using the N-terminal portion of this protein. Only DSC2a WT bound to this protein fragment, no binding of DSC2b was observed. The binding of DSC2 A897fsX900 was weaker in comparison to DSC2a WT (~50%, *Figure 5C*).

3.6 The DSC2 mutations affect desmosomal PG

We observed the loss of PG signal from the ID in the myocardium of an individual (55.2) with the DSC2 G371fsX378 null mutation (*Figure 6A*; other desmosomal components in Supplementary material online, *Figure S5B*). In the absence of patient material for the other mutations, co-immunoprecipitation experiments were performed with full-length DSC2a constructs. In agreement with its non-functional state, binding of DSC2 R203C to PG and PKP2 was reduced (*Figure 6B*). In the case of the DSC2 A897fsX900 variant, binding to PKP2 was comparable to DSC2a WT, while its affinity for PG was again reduced (*Figure 6C*).

In conclusion, we have identified a strong pathogenic potential for the two missense mutations as well as moderate changes for the DSC2 A897fsX900 variant. Moreover, all mutations could potentially affect PG at the ID; however, we failed to detect altered PG localization in NRC transfected with DSC2 R203C or T275M (*Figure 6D*). Our findings suggest that the two missense changes in DSC2 may indeed contribute to the pathogenesis of ARVC and in addition might help to explain why the A897fsX900 variant may not be fully penetrant.

4. Discussion

In the ID of cardiomyocytes, desmosomes provide a rigid connection between neighbouring cells, allowing them to withstand mechanical strain. In these structures, the desmosomal cadherins DSG2 and DSC2 homo- and heterodimerize with their extracellular cadherin domains, whereas their intracellular portions bind other desmosomal components, i.e. PG and PKP2, which in turn link to DSP, which provides a link to the desmin cytoskeleton.[5]

Mutations in these five cardiac desmosomal genes can cause ARVC,[1,2] a disease associated with life-threatening arrhythmias and high incidence of sudden cardiac death. Tissue analysis of Individual

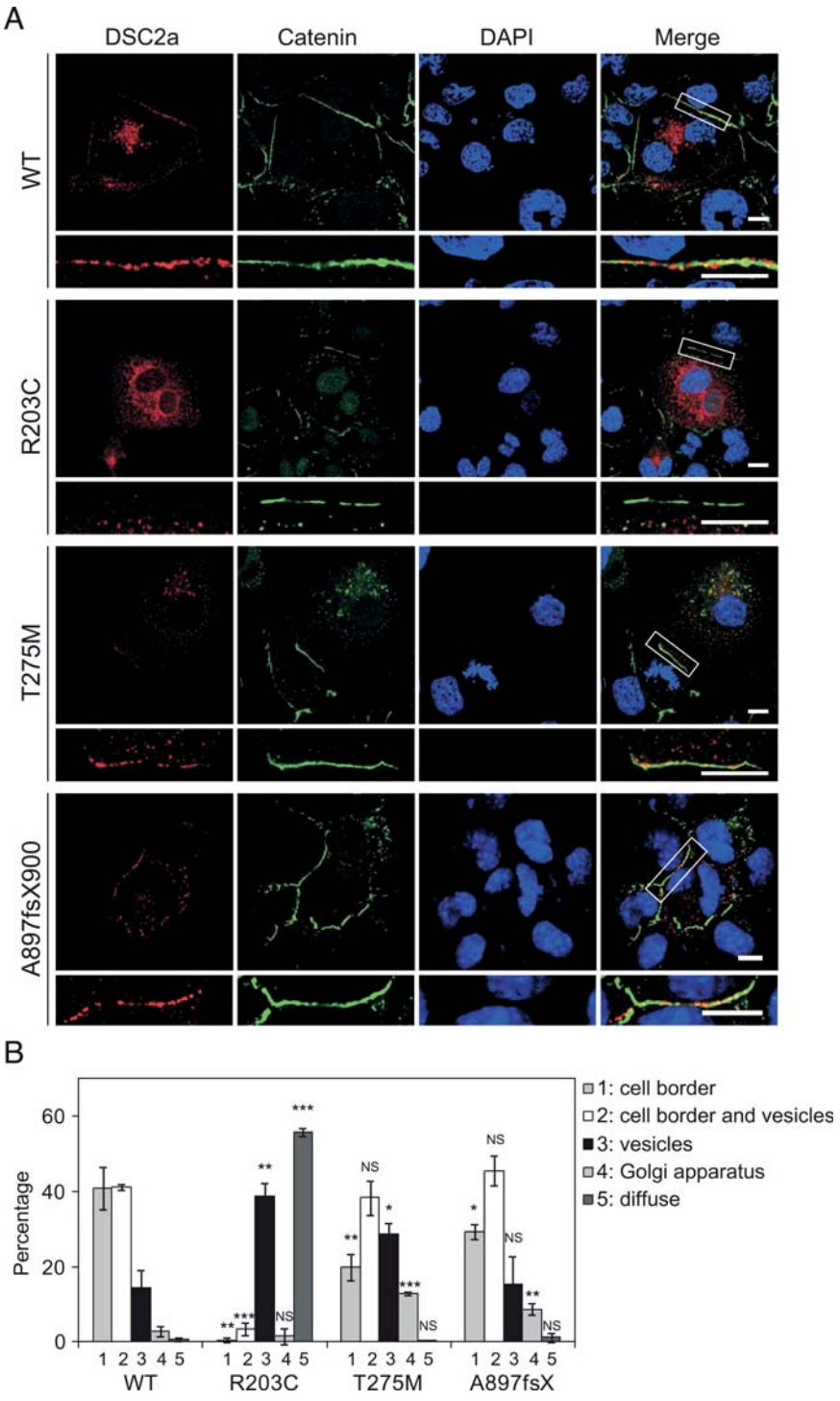

Figure 3 Localization of DSC2 WT, R203C, T275M, and A897fsX900 in HL-1 cells. (*A*) Localization of the DSC2 WT, R203C, T275M, and A897fsX900 proteins in transiently transfected HL-1 cells (red), counterstained with the cell–cell contact marker β-catenin (green), nuclei are visualized with 4′,6-diamidino-2-phenylindole (DAPI, blue), and merged images (forth column). Indicated areas (white boxes) are also shown enlarged below. Scale bars, 10 μm. DSC2 WT and A897fsX900 were primarily found at the desmosomes of cell–cell contacts (with some additional Golgi apparatus and vesicular localization upon higher expression levels); however, DSC2 R203C was completely absent from cell–cell contacts, whereas DSC2 T275M showed less efficient targeting to these structures. (*B*) Quantification of changes in cellular localization. Localization of transfected HL-1 cells was divided into categories 1–5 (for examples of each category, see Supplementary material online, *Figure S6*). Cells (>200 per construct per experiment) were counted and the percentage of each category was calculated. Combined data of three independent experiments are shown. Significant changes in cellular distribution compared with the same category for WT are indicated: $*P < 0.05$, $**P < 0.01$, $***P < 0.001$; NS, not significant.

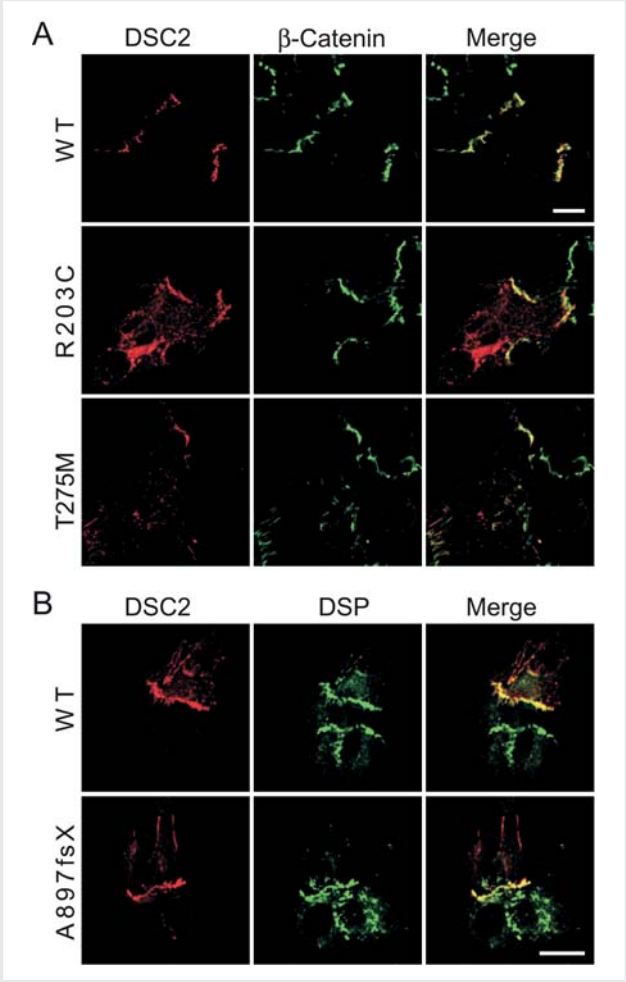

Figure 4 Localization of DSC2 WT, R203C, T275M, and A897fsX900 in NRC. (*A*) Localization of the DSC2 WT (top), R203C (middle), and T275M (bottom) proteins in transfected NRC (red), counterstained with the ID marker β-catenin (green), and merged images (third column). Scale bar 10 μm. DSC2 WT was primarily found at the ID structures. DSC2 R203C showed only marginal targeting to the ID, but was primarily found in vesicles throughout the cytoplasm. DSC2 T275M showed targeting to the ID, but to a lesser extent, and was additionally found in vesicular structures in the cytoplasm. (*B*) Localization of the DSC2 WT (top) and A897fsX900 (bottom) proteins in transfected NRC (red), counterstained with DSP as an ID marker (green), and merged images (third column). Scale bar, 10 μm. The DSC2 A897fsX900 protein is normally targeted to the ID structures.

55.2 provided insights into potential mechanisms underlying arrhythmias and sudden cardiac death: fibrosis (see Supplementary material online, *Figure S5A*) is thought to cause electric isolation of cardiomyocytes and may thereby facilitate reentrant excitation (discussed in Gehmlich *et al.*[13]). In addition, gap junction remodelling (as documented by loss of Cx43 signal from the IDs; see Supplementary material online, *Figure S5B*) may contribute to conduction heterogeneity and increase the risk of arrhythmic events.[13]

Failure of appropriate localization of PG to the ID, irrespective of the underlying genetic mutation, is a recently suggested feature of ARVC.[7] We have confirmed this observation for the first time for a DSC2 mutation (*Figure 6A*). This suggests that PG plays a major role in the pathogenesis of ARVC. The mechanisms of how diverse changes in different desmosomal proteins cause the same disease however are poorly understood.

Here, we explore the consequences of ARVC-associated DSC2 mutations at the molecular level. Any mutation resulting in a premature stop codon before the transmembrane domain is predicted not to produce any functional protein. Such null alleles, e.g. the newly identified DSC2 L229X and DSC2 G371fsX378 mutations, as well as previously reported ones,[15,17] act primarily through haplo-insufficiency, and such a reduction of one desmosomal component is likely to have deleterious effects on the entire structure, as observed by electron microscopy for ARVC patients and DSC2 knockdown in a zebrafish model.[15,28] In particular, 50% reduction of DSC2 at the desmosomes reduces the number of ligands for PG and PKP2 in the structures. DSC2 and DSG2 bind to PG and PKP2 with similar strength (*Figure 5A*), so lack of DSC2 could only be partly compensated by DSG2. In addition, missense mutations in DSC2 can also potentially affect desmosomal structure and integrity.

The two novel missense mutations investigated, DSC2 R203C and DSC2 T275M, are located in the N-terminal cadherin domains. These modules mediate the adhesive properties of the cadherins in a calcium-dependent fashion, and the binding of calcium ions at the interface of neighbouring cadherin domains is a pre-requisite for cadherin function.[29,30] Both affected residues (R203 and T275) are evolutionary conserved and structural models suggest crucial roles of both mutated residues for the domain integrity (see Supplementary material online, *Figure S4B*).

Both mutant proteins exhibit defects in processing into the mature form (*Figure 2*; see Supplementary material online, *Figure S2*). Normally, this proteolytic process involves endoprotein convertases and results in functional activation of DSC2, because in the precursor form, the pro-protein extension prevents binding to other cadherins.[31] In the case of DSC2 R203C, the mutant fails to undergo the complete cleavage, whereas the DSC2 T275M protein can still be processed, but shows a higher pro-protein to mature protein ratio (*Figure 2B* and *C*; see Supplementary material online, *Figure S2*). As a consequence, the non-functional DSC2 R203C fails to localize at the desmosomes of ID structures, whereas only a proportion of the partly functional DSC2 T275M protein is still incorporated into the desmosomes (*Figures 3* and *4*).

In our study, Patient 35.1 is heterozygous for DSC2 R203C and Patient 37.1 is homozygous for DSC2 T275M. In the former, 50% of DSC2 is functional as there is only one DSC2 WT allele present. In the latter, our experiments show that only two-thirds of the DSC2 are processed into the mature form. Consequently, in both cases, there is a significant reduction of the mature, functional DSC2 protein level at the ID. This further implies that lack of functional DSC2 at the ID is primarily responsible for the disease phenotype rather than a dominant-negative action of the mutant proteins. Partially, abnormal localization of two other ARVC-associated DSC2 missense mutations has also been noted in cardiomyocytes.[12]

The properties of the DSC2 A897fsX900 protein contrast with the findings with the N-terminal mutations. This C-terminal mutation changes the last five amino acids of the larger DSC2a splice isoform, whereas the DSC2b isoform is unaffected (see Supplementary material online, *Figure S1A*). Our findings suggest that this mutant protein is normally processed into its mature form and can be incorporated into the desmosomes of HL-1 cells and cardiomyocytes (*Figures 3* and *4*). In contrast to only minor changes in

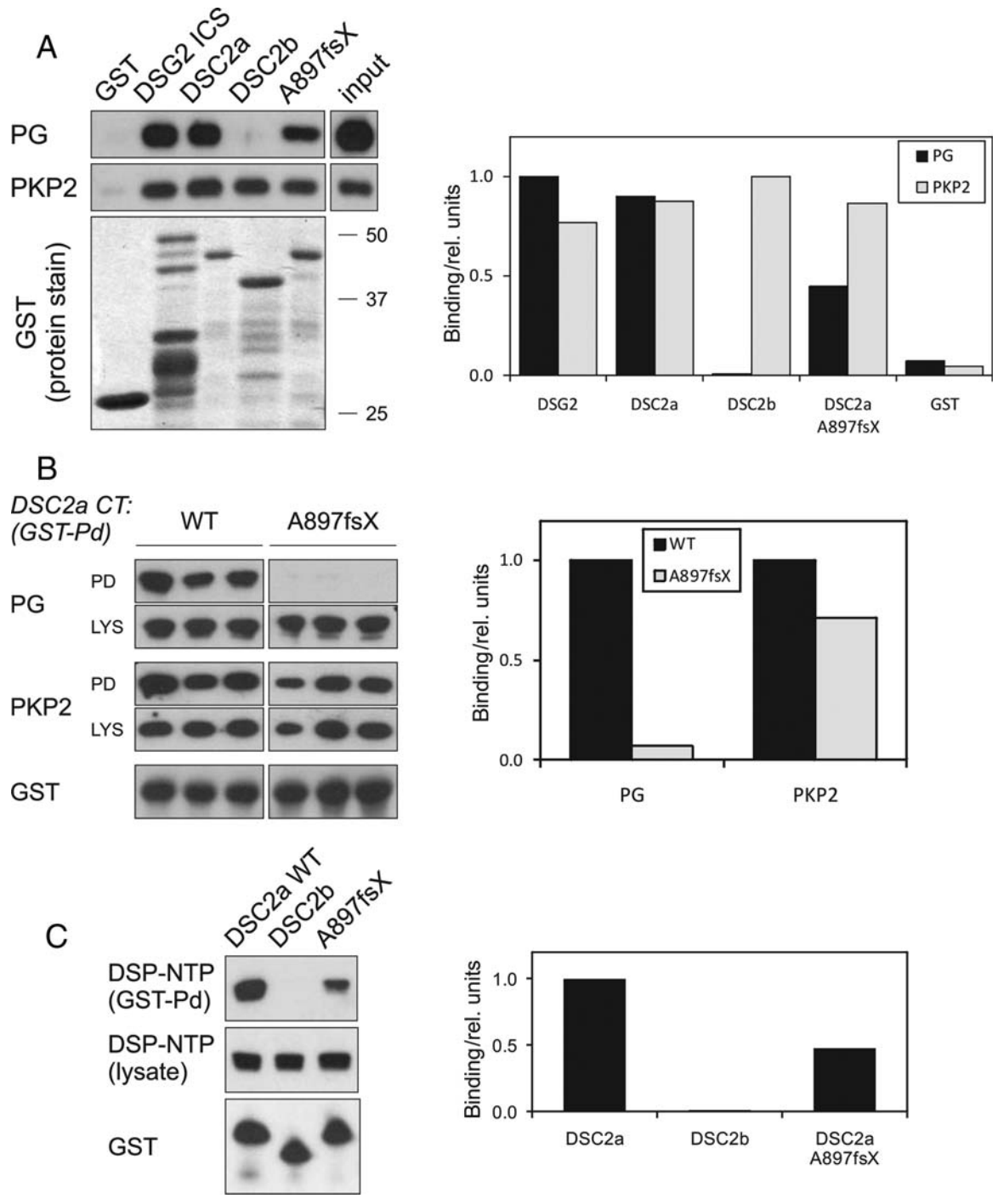

Figure 5 The DSC2a A897fsX900 variant is impaired in binding PG and DSP. (*A*) (Left) Binding of PG and PKP2 to desmosomal cadherins (DSC2a, DSC2b, DSG2, and DSC2a A897fsX900) in GST-pulldown assays. A dilution (1%) of the rat heart lysate is shown ('input'). A Coomassie-stained gel shows the GST fusion protein inputs, together with a GST alone control (the position of the marker proteins is indicated on the right). Note that the DSG2 GST-fusion preparation additionally contains degradation products. (Right) Quantification of the bound protein by densitometry, relative to the strongest interaction (set to 1.0), black columns indicate binding of PG and grey columns of PKP2 to the GST fusion proteins. (*B*) (Left) Reduced binding of DSC2a A897fsX900 cytoplasmic domain to endogenous PG in COS-1 cells. GST fusion proteins of DSC2a WT and A897fsX900 were expressed in COS-1 cells and assayed for binding to PG and PKP2 in GST-pulldown assays (PD). For comparison, lysate controls (LYS) of PG and PKP2, as well as GST-DSC2a proteins are given (GST). (Right) Quantification of the bound PG (black) and PKP2 (grey) protein by densitometry, relative to DSC2a WT (set to 1.0). For the DSC2a A897fsX900 protein, binding to PG was dramatically reduced, whereas binding to PKP2 was only mildly affected. (*C*) (Left) Reduced binding of DSC2a A897fsX900 cytoplasmic domain to DSP. GST fusion proteins of DSC2a WT and A897fsX900 were co-expressed with DSP-NTP (fused to GFP) in COS-1 cells and assayed for binding in GST-pulldown assays (GST-Pd). For comparison, lysate controls for DSP-NTP, as well as GST-DSC2a proteins in the GST pulldown (GST) are given. (Right) Quantification of the bound DSP-NTP by densitometry, relative to DSC2a WT (set to 1.0). Binding of DSC2a A897fsX900 protein to DSP-NTP was reduced to ~50%.

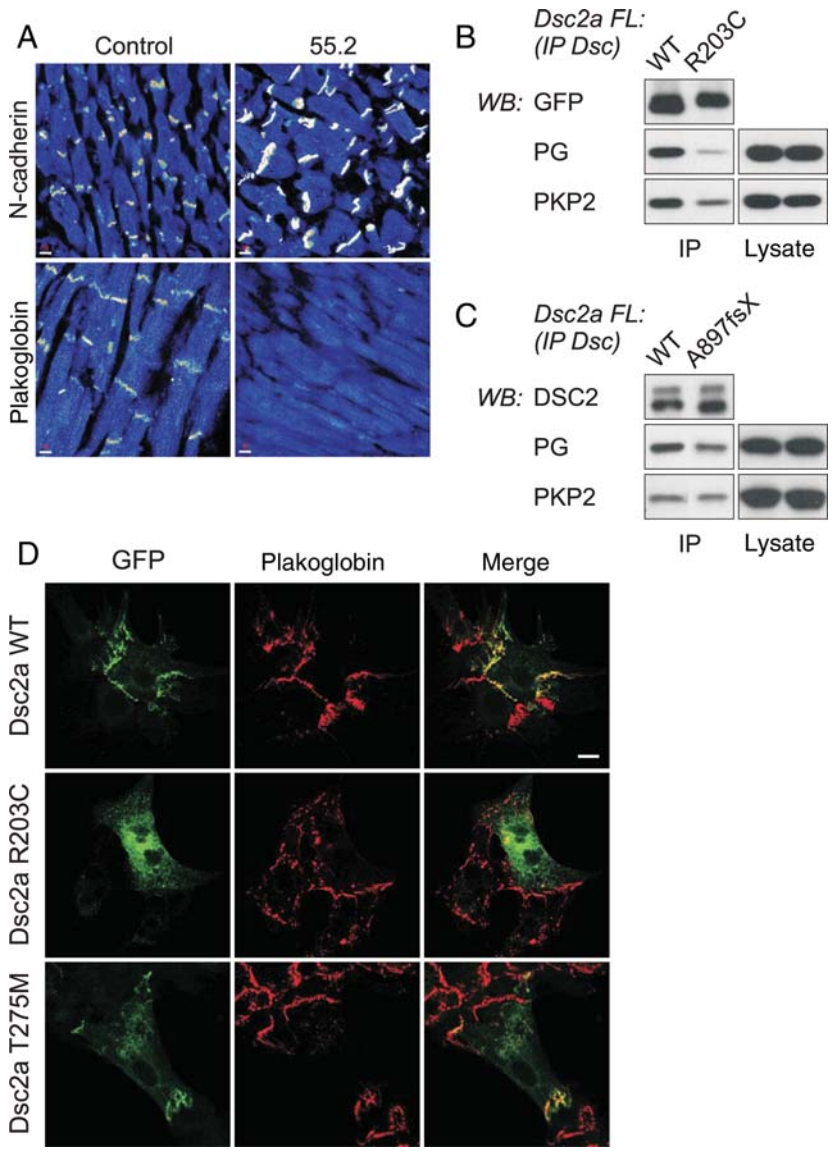

Figure 6 The DSC2a mutations potentially affect PG at the IDs. (*A*) Confocal immunofluorescence analysis of myocardial tissue from Patient 55.2 (heterozygous DSC2 G371fsX378 mutation). The PG signal is strongly reduced at the ID of Patient 55.2 in comparison to non-failing control tissue, whereas the adherens junction protein N-cadherin can be abundantly detected at the IDs of both samples. Scale bar, 10 μm. For staining of other desmosomal proteins, see Supplementary material online, *Figure S5*. (*B*) Reduced binding of DSC2a R203C to PG and PKP2 in COS-1 cells. Transfected full-length DSC2a WT or R203C GFP was immunoprecipitated with a DSC2 antibody and bound PG and PKP2 detected; cell lysates are also shown. (*C*) Reduced binding of DSC2a A897fsX900 to PG, but not to PKP2 in COS-1 cells. Transfected full-length DSC2a WT or R203C (tag-free proteins) was immunoprecipitated as in (*B*) and bound PG and PKP2 detected; cell lysates are also shown. (*D*) PG localization (red) in NRCs expressing DSC2a WT, R203C, and T275M (green). Scale bar represents 10 μm. In all three transfections, PG was found at the ID, regardless of the localization of the DSC2 GFP fusion protein; the abundance of endogenous DSC2 WT protein may compensate any deleterious effect of the DSC2 mutants.

localization observed in our experiments (*Figure 3*), a recent report by De Bortoli *et al.*[18] suggested the mis-localization of this variant in HL-1 cells. The use of a GFP fusion protein construct in their experiments might artificially have obscured the real localization of the mutant protein. We utilized the lack of cross-reactivity of our antibodies with rodent proteins to study the behaviour of non-tagged human constructs (exposing the different carboxy-termini) and found only small changes in cellular localization.

Our GST-pulldown assays clearly demonstrate impaired binding of the DSC2a A897fsX900 variant to PG and DSP (*Figure 5*), while binding to PKP2 was virtually unaffected. This finding was confirmed by co-immunoprecipitation experiments using full-length proteins. As observed before, the DSC2 A897fsX900 protein bound more weakly to PG than DSC2a WT, while binding to PKP2 was normal (*Figure 6C*). However, the effect seen here was not as dramatic as in experiments using only the cytoplasmic portion, and this may be explained by potential homo- or heterodimerization with desmosomal cadherins via the N-terminal cadherin domains.[30]

The DSC2 A897fsX900 variant has now been found in apparently healthy individuals.[18] Although a low expression level of the DSC2a

isoform in the myocardium[18] may contribute to the lack of an overt phenotype in these individuals, our functional studies demonstrate a pathogenic potential of this variant: its impaired binding to PG cannot directly be compensated by the DSC2b isoform, which does not bind PG (*Figure 5A*). However, the cytoplasmic domain of DSG2 appears to have redundant functions in binding PG in the desmosomes. Currently, it is unclear whether carriers of the variant exhibit subclinical features of disease expression or what the potential is for disease development in individuals who perform endurance training or carry other common variants. In the future, high-throughput genomic analysis of large families and large, well-defined cohorts might help to answer these questions.

The striking observation of our functional studies is that—despite their different individual properties—all the DSC2 mutant proteins appear to affect PG at the IDs: for each of the mutations, the ability of DSC2 to provide an anchor for PG is impaired. As a consequence, PG may not be efficiently targeted to, or retained at, the desmosomes, and in turn might become available for other intracellular pools. This loss of PG from the ID has been reported in ARVC patients[7] (including individuals with DSC2 mutations, *Figure 6A*). Beyond being a diagnostic feature, this event may be crucial in disease pathogenesis: data from transgenic animal studies suggest that unbound PG might be translocated into the nucleus and could aberrantly modulate transcriptional pathways, especially by competing with β-catenin in the Wnt-signalling pathways.[8,11] Our functional studies on the three DSC2 mutations suggest for the first time a molecular explanation how DSC2 mutations may contribute to the same 'common final pathway' of ARVC.

In transfection experiments, we failed to observe a redistribution of PG from the ID in the presence of the mutant DSC2 proteins (*Figure 6D*), neither were changes in desmosomal composition observed (see Supplementary material online, *Figure S2*). However, these cellular systems may not be adequate to reflect the *in vivo* situation: in patients with heterozygous mutations, one functional WT allele is replaced by a mutant DSC2 form, which affects PG binding. In contrast, the mutant DSC2 proteins were expressed in addition to the endogenous DSC2 in our experiments. Therefore, the abundant endogenous DSC2 protein may compensate any deleterious effects of the DSC2 mutants. As demonstrated for mutations in the cytoplasmic region of DSG2,[13] additional indirect effects beyond altered binding properties may contribute to the complexity of the disease.

In the future, the reduction of functional DSC2 protein in a cellular model systems (e.g. by RNA interference) will be a valuable tool to study down-stream pathogenic events, such as the redistribution of PG from the ID and aberrant activation of PG signalling in the nucleus. Moreover, animal models engineered for the cardiac-specific expression of DSC2 mutation forms will help to provide mechanistic insights into ARVC.

Supplementary material

Supplementary material is available at *Cardiovascular Research* online.

Acknowledgements

We thank Prof. Werner Franke (Heidelberg, Germany), Alan Whitmarsh (Manchester, UK) and Ross Breckenridge (London, UK) for donation of reagent. We would like to acknowledge the technical support of Dennis Sadic, Thomas Cahill and Mareike Reimann.

Conflict of interest: none declared.

Funding

This work was supported by the British Heart Foundation (RG/04/010 to W.J.M.), the National Institute of Health (to J.E.S.) and the Heart Rhythm Society (to A.A.). This work was undertaken at University College London/Hospital which received a proportion of funding from the Department of Health's National Institute for Health Research Biomedical Research Centres. Funding to pay Open Access publication charge was provided by the British Heart Foundation.

References

1. Ahmad F. The molecular genetics of arrhythmogenic right ventricular dysplasia-cardiomyopathy. *Clin Invest Med* 2003;**26**:167–178.
2. Awad MM, Calkins H, Judge DP. Mechanisms of disease: molecular genetics of arrhythmogenic right ventricular dysplasia/cardiomyopathy. *Nat Clin Pract Cardiovasc Med* 2008;**5**:258–267.
3. Thiene G, Corrado D, Basso C. Arrhythmogenic right ventricular cardiomyopathy/dysplasia. *Orphanet J Rare Dis* 2007;**2**:45.
4. Dusek RL, Godsel LM, Green KJ. Discriminating roles of desmosomal cadherins: beyond desmosomal adhesion. *J Dermatol Sci* 2007;**45**:7–21.
5. Green KJ, Simpson CL. Desmosomes: new perspectives on a classic. *J Invest Dermatol* 2007;**127**:2499–2515.
6. Corrado D, Basso C, Thiene G, McKenna WJ, Davies MJ, Fontaliran F *et al.* Spectrum of clinicopathologic manifestations of arrhythmogenic right ventricular cardiomyopathy/dysplasia: a multicenter study. *J Am Coll Cardiol* 1997;**30**:1512–1520.
7. Asimaki A, Tandri H, Huang H, Halushka MK, Gautam S, Basso C *et al.* A new diagnostic test for arrhythmogenic right ventricular cardiomyopathy. *N Engl J Med* 2009;**360**:1075–1084.
8. Garcia-Gras E, Lombardi R, Giocondo MJ, Willerson JT, Schneider MD, Khoury DS *et al.* Suppression of canonical Wnt/beta-catenin signaling by nuclear plakoglobin recapitulates phenotype of arrhythmogenic right ventricular cardiomyopathy. *J Clin Invest* 2006;**116**:2012–2021.
9. Joshi-Mukherjee R, Coombs W, Musa H, Oxford E, Taffet S, Delmar M. Characterization of the molecular phenotype of two arrhythmogenic right ventricular cardiomyopathy (ARVC)-related plakophilin-2 (PKP2) mutations. *Heart Rhythm* 2008;**5**:1715–1723.
10. Kirchhof P, Fabritz L, Zwiener M, Witt H, Schafers M, Zellerhoff S *et al.* Age- and training-dependent development of arrhythmogenic right ventricular cardiomyopathy in heterozygous plakoglobin-deficient mice. *Circulation* 2006;**114**:1799–1806.
11. Lombardi R, Dong J, Rodriguez G, Bell A, Leung TK, Schwartz RJ *et al.* Genetic fate mapping identifies second heart field progenitor cells as a source of adipocytes in arrhythmogenic right ventricular cardiomyopathy. *Circ Res* 2009;**104**:1076–1084.
12. Beffagna G, De BM, Nava A, Salamon M, Lorenzon A, Zaccolo M *et al.* Missense mutations in desmocollin-2 N-terminus, associated with arrhythmogenic right ventricular cardiomyopathy, affect intracellular localization of desmocollin-2 *in vitro*. *BMC Med Genet* 2007;**8**:65.
13. Gehmlich K, Asimaki A, Cahill T, Ehler E, Syrris P, Zachara E *et al.* Novel missense mutations in exon 15 of desmoglein-2: Role of the intracellular cadherin segment in arrhythmogenic right ventricular cardiomyopathy. *Heart Rhythm* 2010;**7**:1446–1453.
14. Pilichou K, Remme CA, Basso C, Campian ME, Rizzo S, Barnett P *et al.* Myocyte necrosis underlies progressive myocardial dystrophy in mouse dsg2-related arrhythmogenic right ventricular cardiomyopathy. *J Exp Med* 2009;**206**:1787–1802.
15. Heuser A, Plovie ER, Ellinor PT, Grossmann KS, Shin JT, Wichter T *et al.* Mutant desmocollin-2 causes arrhythmogenic right ventricular cardiomyopathy. *Am J Hum Genet* 2006;**79**:1081–1088.
16. Lorimer JE, Hall LS, Clarke JP, Collins JE, Fleming TP, Garrod DR. Cloning, sequence analysis and expression pattern of mouse desmocollin 2 (DSC2), a cadherin-like adhesion molecule. *Mol Membr Biol* 1994;**11**:229–236.
17. Syrris P, Ward D, Evans A, Asimaki A, Gandjbakhch E, Sen-Chowdhry S *et al.* Arrhythmogenic right ventricular dysplasia/cardiomyopathy associated with mutations in the desmosomal gene desmocollin-2. *Am J Hum Genet* 2006;**79**:978–984.
18. De Bortoli M, Beffagna G, Bauce B, Lorenzon A, Smaniotto G, Rigato I *et al.* The p.A897KfsX4 frameshift variation in desmocollin-2 is not a causative mutation in arrhythmogenic right ventricular cardiomyopathy. *Eur J Hum Genet* 2010;**18**:776–782.
19. Sen-Chowdhry S, Syrris P, McKenna WJ. Role of genetic analysis in the management of patients with arrhythmogenic right ventricular dysplasia/cardiomyopathy. *J Am Coll Cardiol* 2007;**50**:1813–1821.
20. Marcus FI, McKenna WJ, Sherrill D, Basso C, Bauce B, Bluemke DA *et al.* Diagnosis of arrhythmogenic right ventricular cardiomyopathy/dysplasia: proposed modification of the task force criteria. *Circulation* 2010;**121**:1533–1541.

21. Saffitz JE, Green KG, Kraft WJ, Schechtman KB, Yamada KA. Effects of diminished expression of connexin43 on gap junction number and size in ventricular myocardium. *Am J Physiol Heart Circ Physiol* 2000;**278**:H1662–H1670.
22. Mayer BJ, Hirai H, Sakai R. Evidence that SH2 domains promote processive phosphorylation by protein-tyrosine kinases. *Curr Biol* 1995;**5**:296–305.
23. Linstedt AD, Hauri HP. Giantin, a novel conserved Golgi membrane protein containing a cytoplasmic domain of at least 350 kDa. *Mol Biol Cell* 1993;**4**:679–693.
24. Lange S, Himmel M, Auerbach D, Agarkova I, Hayess K, Fürst DO *et al*. Dimerisation of myomesin: implications for the structure of the sarcomeric M-band. *J Mol Biol* 2005; **345**:289–298.
25. Barahona-Dussault C, Benito B, Campuzano O, Iglesias A, Leung TL, Robb L *et al*. Role of genetic testing in arrhythmogenic right ventricular cardiomyopathy/dysplasia. *Clin Genet* 2010;**77**:37–48.
26. den Haan AD, Tan BY, Zikusoka MN, Llado LI, Jain R, Daly A *et al*. Comprehensive desmosome mutation analysis in North Americans with arrhythmogenic right ventricular dysplasia/cardiomyopathy. *Circ Cardiovasc Genet* 2009;**2**:428–435.
27. Gloushankova NA, Wakatsuki T, Troyanovsky RB, Elson E, Troyanovsky SM. Continual assembly of desmosomes within stable intercellular contacts of epithelial A-431 cells. *Cell Tissue Res* 2003;**314**:399–410.
28. Basso C, Czarnowska E, Della BM, Bauce B, Beffagna G, Wlodarska EK *et al*. Ultrastructural evidence of intercalated disc remodelling in arrhythmogenic right ventricular cardiomyopathy: an electron microscopy investigation on endomyocardial biopsies. *Eur Heart J* 2006;**27**:1847–1854.
29. Pertz O, Bozic D, Koch AW, Fauser C, Brancaccio A, Engel J. A new crystal structure, Ca^{2+} dependence and mutational analysis reveal molecular E-details of cadherin homoassociation. *EMBO J* 1999;**18**:1738–1747.
30. Syed SE, Trinnaman B, Martin S, Major S, Hutchinson J, Magee AI. Molecular interactions between desmosomal cadherins. *Biochem J* 2002;**362**:317–327.
31. Koch AW, Farooq A, Shan W, Zeng L, Colman DR, Zhou MM. Structure of the neural (N-) cadherin prodomain reveals a cadherin extracellular domain-like fold without adhesive characteristics. *Structure* 2004;**12**:793–805.